

Order Parameter and Density Effects in the Third-Order Nonlinear Optical Properties of Liquid Crystals

Masahide Terazima

Department of Chemistry, Graduate School of Science, Kyoto University, Kyoto 606

(Received January 23, 1996)

Third-order nonlinear optical effects induced by thermal and photochemical reactions after a real photoexcitation of neat (undoped) liquid crystals (*N*-(4-methoxybenzylidene)-4-butaniline (MBBA) and cyanopentylbiphenyl) were investigated by the transient grating method with nanosecond and picosecond pulsed-laser systems. The origins of the effect were clearly separated into the density and order parameter changes by a polarization selection of the probe beam; also, the dynamics (speed of the changes) of both components were investigated. The decrease in the density under the presence of the *cis* form of MBBA was observed and could be explained in terms of a void volume effect.

Compared with isotropic fluids, liquid crystals are very unique materials concerning many physical properties.¹⁾ One of the unique optical properties is an extraordinarily large nonlinear optical effect, which has attracted many scientists in a variety of aspects for both fundamental and applicational purposes.^{2–15)} These nonlinearities are caused by a strong light-matter interaction, and have been studied by many methods such as self-(de)focusing, optical phase conjugation, self oscillation, cross phase modulation, the four wave mixing techniques and so on. When the pumping light is nonresonant to any real excited states, the optical Kerr effect (electronic and orientational responses)¹⁶⁾ and electrostriction are the main origins of the nonlinearity. After real photoexcitation to the electronic excited states of the liquid crystal molecules, a very large optical nonlinearity is observed, which is induced by the thermal effect from the nonradiative transition or photochemical reactions. This nonlinear optical effect increases dramatically near the phase transition temperature, which suggests that the origin of the nonlinearity is the density effect as well as the order parameter.^{3,5–8,10)} However, studies concerning the nonlinear optical effect with a clear separation of these origins have been very scarce.

In this study, the relative contributions of the density and the order parameter changes at various temperatures after real photoexcitation of liquid crystals, *N*-(4-methoxybenzylidene)-4-butaniline (MBBA) and cyanopentylbiphenyl (5CB), was investigated by using the transient grating (TG) method with a polarization selection of a probe beam from a picosecond to millisecond time scale. By choosing a proper direction of the probe polarization, the relative intensities as well as the temporal profiles for both contributions could be studied independently.

After the photoexcitation of MBBA, the molecule isomerizes from the *trans* form to the *cis* form and the isomerization produces an additional nonlinear optical effect.^{13,15)} From a

polarization selection experiment, it is shown that the density of the liquid crystal is changed due to the creation of the *cis* form, even without a temperature change. The dynamics of the density and the order parameter have also been studied for 5CB by observing the light-induced acoustic signal using the TG method with picosecond and nanosecond laser excitation.

Experimental

The experimental setup for the TG measurement was similar to that reported previously.^{15,17)} A laser beam from an excimer laser-pumped dye laser (Lumonics Hyper 400, Hyper Dye 300; wavelength, 390 nm) was used as the excitation light for MBBA and the third harmonics of a Nd:YAG laser for 5CB. Since both excitation wavelengths were on long wavelength tails of the absorption bands of MBBA and 5CB, this ensured that the excitation was uniform across the sample. These beams were split into two with a beam splitter, and intersected inside a sample to create a transient grating. The sample was sandwiched between two glass plates, which were coated with a thin film of poly(vinyl alcohol) and rubbed unidirectionally to achieve a homogeneous alignment. The sample thickness was about 50 μm . A linearly polarized CW laser beam was used as a probe beam, and the polarized beam was produced from an unpolarized He-Ne laser with a sheet polarizer. The probe beam was brought into the TG region at an angle that satisfied the Bragg condition. The diffracted signal was detected by a photomultiplier and averaged by a digital oscilloscope (Tektronix 2430A) and a microcomputer. The polarization of the TG signal was selected by another sheet polarizer placed before the detector. The extinction ratio of the polarizers was better than 10^{-3} . When linearly polarized light passes through an optically uniaxial material, it is converted to the ellipsoidally polarized light except a case that the direction of the polarization matches to the optical axis.¹⁸⁾ The polarization after the liquid crystal samples was verified not to be rotated by properly choosing the direction of the extraordinary or ordinary ray to the liquid crystal sample. The extinction ratio after passing through the unidirectionally oriented liquid crystal sample was ca. 10^{-2} ; the smaller ratio than that without the sample may have been due to an

imperfect alignment of the sample by our rubbing method.

The sample was temperature controlled by a heated aluminum holder, and the temperature was measured by a copper-constantan thermo-couple. The laser power of the excitation light was kept as low as possible for the measurement. This power depended on the sample temperature, because the signal intensity is a very strong function of the temperature as described later. It is typically less than 0.2 mJ cm^{-2} at room temperature, and much weaker at higher temperatures. When the laser power was sufficiently low, the TG signal of MBBA consists of the thermal grating and population grating, whose lifetimes were determined by the thermal conduction and mass diffusion between the fringe spacing, respectively (Fig. 1(a) and next Section 1). However, if the laser power became higher, an additional signal having a slower rise and an intermediate decay rate between the thermal and population grating signals appeared (Fig. 1(b)). At present, we do not know the exact origin of this slower rise and additional decay in the signal. These rise and decay rates were sensitive to the laser power, and this signal was avoided in the measurement by keeping the laser power low.

For a picosecond experiment, the third harmonics of a Nd : YAG laser (Contium, PY61c-10) was used for the pump laser and the second harmonics-pumped dye laser pulse (640 nm) was used for the probe beam. The pulse width of both beams was ca. 30 ps. The excitation beams were crossed inside the sample at a relatively large angle (30°) to achieve a short build-up time of the acoustic signal. The probe pulse was optically delayed against the pump pulse by a mechanical translational stage, and the TG signal detected by a photomultiplier and a boxcar integrator was plotted against the delay time. 5CB gradually photodegraded upon photoexcitation at 355 nm. The sample was slowly translated by a mechanical translational stage during photoirradiation to monitor the optical nonlinearity from a fresh sample. The signal averaging of this sample was also kept as a small number shots as possible.

MBBA (Tokyo Kasei Co.) and 5CB (Aldrich) were used without further purification.

Results and Discussion

1. Origin of the Thermal Grating of MBBA. A typical TG signal after the photoexcitation of MBBA in the nematic phase is shown in Fig. 1. According to the theory of the volume grating,¹⁹⁾ the TG signal intensity is proportional to the square of the refractive index change if the absorption at the probe wavelength is negligible (such as in this case). The square root of the TG signal of MBBA can be represented by a sum of two exponential functions (Fig. 1). The faster decay component is the thermal grating signal, whose decay rate is determined by the thermal conduction between the fringes; the slower one is due to the presence of the cis form (the population grating), which is created by the photoisomerization reaction of the trans form of MBBA.^{13,15)} The lifetime of the population grating represents the diffusion process of MBBA between the fringes.

A similar TG signal was observed from a sample of MBBA in an ethanol solution (isotropic fluid). The refractive index change of the thermal grating in an isotropic fluid has been extensively studied and the thermal grating signal is attributed to a density change of the matrix due to the thermal energy that comes out from the radiationless transition.^{17,19)} The origin of the population grating in this case is attributed to

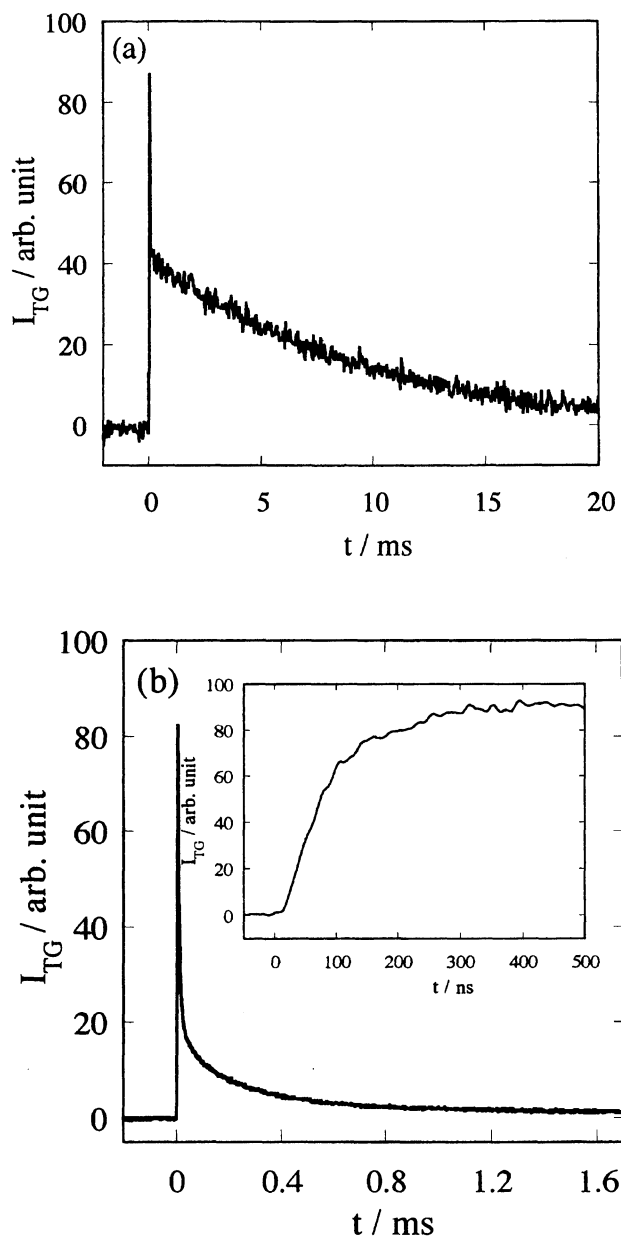


Fig. 1. (a) Typical TG signal after the photoexcitation of MBBA with a weak excitation laser (ca. 0.1 mJ cm^{-2}) and (b) with a stronger laser power (ca. 1 mJ cm^{-2}) at the room temperature. At the weak laser power, the signal consists of only the thermal grating signal (initial spike-like signal) and population grating signal (slowly decaying signal), while another type of intermediate signal appears (0–0.4 ms) at the stronger laser power. The inset in (b) shows the rise curve under the same laser power condition. The build up time under the weak laser power is sufficiently fast in this time scale as shown in Fig. 5.

the different polarizabilities between the cis and trans forms. However, there are several different characteristic features in the TG signal in the nematic phase. For example, the relative intensity of the population grating signal (to the thermal grating signal) is much stronger in the nematic phase. Second, the intensities of the both components increase divergently

as the temperature approaches the phase transition to the isotropic phase and they suddenly drop by about two to three orders of magnitude above the phase transition (in isotropic phase). A similar temperature dependence has been reported for some liquid crystals.^{3,4c,7,8,15)} These characteristic features indicate that the origin of the TG signal is not the same as those of isotropic fluids.

We first studied the origin of the thermal grating signal. After photoexcitation to the electronic excited state of MBBA, it relaxes back to the ground state mainly through the radiationless transition. As the energy is released as heat to the surrounding matrix, it raises the temperature. Several studies have demonstrated that the change in the refractive index because of the thermal energy is due to a change in several factors.^{3–12)} The most significant contribution comes from the density (ρ) and the order parameter (S),^{4a)} which can be given by three terms as

$$\delta n^{\text{th}} = \left\{ \left(\frac{\partial n}{\partial T} \right)_{\rho} + \left(\frac{\partial n}{\partial \rho} \right)_{\text{T}} \left(\frac{\partial \rho}{\partial T} \right) + \left(\frac{\partial n}{\partial S} \right)_{\rho} \left(\frac{\partial S}{\partial T} \right) \right\} \delta T. \quad (1)$$

The first term is due to the refractive index change due to the temperature rise without a density change. The second term is the refractive index variation through a density change, which results from a thermal expansion of the medium. The last term represents the effect of the order parameter, which is a function of the temperature. We have shown that the magnitude of the first term is about one order of magnitude smaller than that of the second term in many fluids (except in water at low temperatures).²⁰⁾ In this paper the sum of the first and the second terms is represented as the ρ contribution ($\delta n_{\rho}^{\text{th}}$) and the last term as the S contribution (δn_S^{th}). One of the significant differences between $\delta n_{\rho}^{\text{th}}$ and δn_S^{th} is that the former contribution is mainly induced by a volume expansion, which leads to a characteristic oscillation in the TG signal, while the latter is not (Section 3).

These two contributions ($\delta n_{\rho}^{\text{th}}$ and δn_S^{th}) can be separately studied by the polarization selection method as follows. An important factor for the liquid crystals is the polarization of the probe light. The nematic phase of MBBA is an uniaxial system, and the refractive index depends on the direction of the polarization. The longitudinal (extraordinary) and transverse (ordinary) components of the refractive index are represented by

$$\begin{aligned} \delta n_e^{\text{th}} &= (\delta n_{\rho}^{\text{th}})_e + (\delta n_S^{\text{th}})_e, \\ \delta n_o^{\text{th}} &= (\delta n_{\rho}^{\text{th}})_o + (\delta n_S^{\text{th}})_o, \end{aligned} \quad (2)$$

where subscripts e and o denote the extraordinary and ordinary light, respectively. The density contribution comes from the thermal expansion of the medium and is given by^{19b)}

$$\begin{aligned} (\delta n_{\rho}^{\text{th}})_{e(o)} &= \frac{\alpha_{e(o)} \Delta H}{C_p \rho} \left(\frac{\partial n}{\partial \rho} \right)_{e(o)} \\ &\propto \frac{\alpha_{e(o)} \Delta H}{C_p \rho} n_{e(o)} \delta \rho, \end{aligned} \quad (3)$$

where α , ΔH , and C_p stand for the thermal expansion coefficient, thermal energy due to the radiationless transition, and

the heat capacity with a constant pressure, respectively. We use the Lorentz–Lorenz relation for the last relation. (Besides the thermal effect, the density change can be induced by the electrostriction effect. However, this effect can be neglected under our low excitation laser power.) Since the refractive index decreases with decreasing the density, we expect that

$$(\delta n_{\rho}^{\text{th}})_{e(o)} < 0. \quad (4)$$

The expression for the refractive index change due to the S contribution can be derived from the molecular polarizability. When a molecule has a cylindrical symmetry, the optical polarizabilities parallel and perpendicular to the molecular axis, which are expressed by $\alpha_{//}$ and α_{\perp} , respectively, have the following relationship:

$$\bar{\alpha} = \frac{1}{3}(\alpha_{//} + 2\alpha_{\perp}), \quad (5)$$

where $\bar{\alpha}$ is the mean polarizability, and the anisotropic part of each α (α^{aniso}) is given by

$$\alpha_{//}^{\text{aniso}} = -2\alpha_{\perp}^{\text{aniso}}. \quad (6)$$

The macroscopic refractive index from a uniaxially oriented sample (such as nematic liquid crystals) has a similar relation, as

$$(\delta n_S^{\text{th}})_e = -2(\delta n_S^{\text{th}})_o, \quad (7)$$

where we assume that the difference between n_e and n_o is small. When the temperature increases, the order parameter decreases leading to a decrease in n_e ; i.e. $(\delta n_S^{\text{th}})_e < 0$ and $(\delta n_S^{\text{th}})_o > 0$. In many cases, the refractive index change due to S is larger than that of ρ and, as a result, $(\frac{\partial n}{\partial T})_e < 0$ and $(\frac{\partial n}{\partial T})_o > 0$ holds.^{1,4a,5,10,11)} If the refractive index change comes from the effect of the order parameter predominantly, the ratio of δn_o and δn_e ($R = \delta n_e / \delta n_o$) should be equal to 2. When the $\delta n_{\rho}^{\text{th}}$ term cannot be neglected, R should increase, because the $\delta n_{\rho}^{\text{th}}$ term is additive to $(\delta n_S^{\text{th}})_e$, but subtractive for $(\delta n_S^{\text{th}})_o$.

Figure 2(a) shows the TG signal probed by the ordinary light (the o-signal) and by the extraordinary light (the e-signal) at 30 °C. The decaying signal in this time scale is due to the thermal grating, and the constant offset is due to the population grating. The decay rate constant of the o-signal and that of the e-signal was the same within an experimental uncertainty. Clearly, from the figure, the ratio of the thermal grating ($R^{\text{th}} = \delta n_e^{\text{th}} / \delta n_o^{\text{th}}$) is much larger than 2 around these lower temperatures. Similar observations have been reported for other liquid crystals: A much weaker TG signal for the ordinary beam than that for extraordinary beam.^{8a)} This value larger than 2 indicates that the thermal grating is composed of the $\delta n_{\rho}^{\text{th}}$ and δn_S^{th} with a comparable magnitude.

The ratio R^{th} approaches 2 as the temperature becomes closer to the phase transition temperature (Fig. 2(b)); it is plotted against the temperature in Fig. 3. The fact that this value approaches 2 can be explained in terms of the increase of the S contribution in the TG signal. From relations (2) and (7) and the observed R^{th} , the relative contribution of ρ and S (ρ/S) at each temperature is calculated and plotted in Fig. 3(b). Here, we assume that $\delta n_{\rho}^{\text{th}}$ for the e-light is

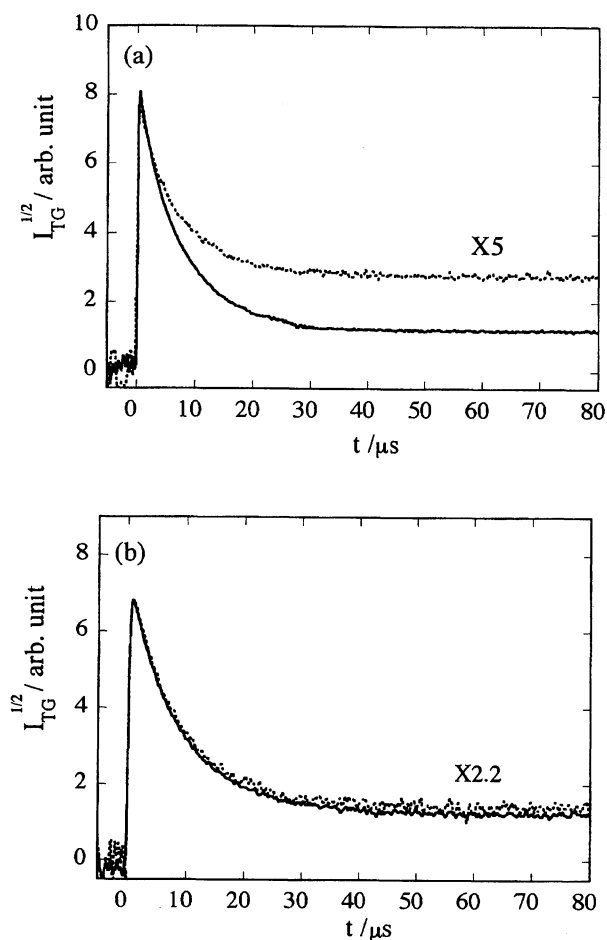


Fig. 2. Typical temporal profiles of the e-signal (solid line) and the o-signal (dotted line) at (a) 30 °C and (b) 45 °C. The constant component in this time scale is the population grating signal.

equal to that for the o-light ($(\delta n_\rho^{\text{th}})_e = (\delta n_\rho^{\text{th}})_o$). Although we have to take into account the difference for a more exact treatment, we expect that the difference is small based on the rather flexible and movable character of the liquid crystals. With increasing the temperature, the S contribution becomes dominant as expected from the theory of liquid crystals.^{1,3)} To my knowledge, this is the first clear and quantitative separation of the ρ and S contributions in the thermal induced nonlinear optical effect.

2. Origin of the Population Grating of MBBA. For MBBA, the slowly decaying TG signal appears after the thermal grating signal, and is attributed to the population grating due to the presence of the cis form. The divergent increase in the population grating intensity indicates that the origin of this signal also comes from the change of S ; that is, the presence of the bended cis form disturbs the ordering of the (rather linear) trans form of MBBA in the nematic phase. This mechanism for the TG signal was indeed verified experimentally by comparing the population grating intensity of a well-aligned sample with that of a previous randomly oriented sample.¹⁵⁾ On the basis of these previous studies, the contribution (δn^{pop}) can be expressed by

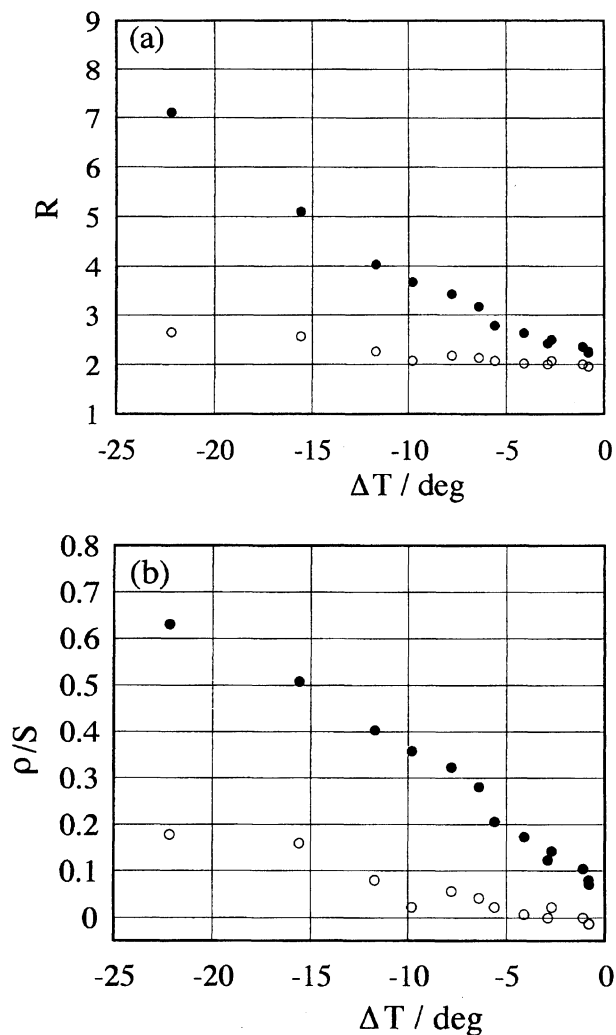


Fig. 3. (a) The ratio (R) of the intensities of the e- and o-signals of the thermal grating (solid circles) and the population grating signals (open circles) at various temperatures. ($\Delta T = T - T_c$, where T_c is the temperature of the nematic-isotropic phase transition) (b) The relative contribution of ρ and S calculated with Eqs. 2 and 7.

$$\delta n^{\text{pop}} = \left\{ \left(\frac{\partial n}{\partial C} \right)_s + \left(\frac{\partial n}{\partial S} \right) \left(\frac{\partial S}{\partial C} \right) \right\} \delta C, \quad (8)$$

where C is the concentration of the cis form induced by the photoisomerization reaction of MBBA. The first term represents the refractive index change due to the different molecular polarizability between the cis and trans forms. The second term indicates the fact that the presence of the cis form disturbs the order of the liquid crystal molecules (changes the order parameter), and then changes the refractive index. Considering the fact that the signal intensity of the population grating in an isotropic fluid is much weaker than that in the nematic phase, we find that the contribution of the second term should be much larger than that of the first term. Previously, this effect was explained in terms of the photostimulated change of the phase transition temperature in the presence of a photoinduced 'impurity' in the nematic phase.³⁾

If the change in S comes only from a disturbance of S by the presence of the cis form, as previously suggested,¹⁵⁾ $R^{\text{pop}} = (\delta n^{\text{pop}})_e / (\delta n^{\text{pop}})_o$ should be 2 as suggested from Eq. 7. It is interesting to note, however, that R^{pop} is close to 2, but slightly larger than that value at low temperatures (Fig. 3). Therefore, although the disorder of the alignment by the presence of the cis form (the S contribution) is the dominant contribution in δn , this fact shows that it is not the only origin. We consider that the other contribution is a density change due to the presence of the cis form (Fig. 4); that is, the refractive index change should be written as

$$\delta n^{\text{pop}} = \left\{ \left(\frac{\partial n}{\partial C} \right)_S + \left(\frac{\partial n}{\partial S} \right) \left(\frac{\partial S}{\partial C} \right) + \left(\frac{\partial n}{\partial \rho} \right) \left(\frac{\partial \rho}{\partial C} \right) \right\} \delta C. \quad (9)$$

It has been considered that the molecular volume in solutions is composed of the intrinsic volume and the other contributions, such as the electrostriction. If the van der Waals volume is defined by the volume occupied by the solute molecule itself as the Bondis's manner,²¹⁾ it can be calculated from functional groups which are the covalently bonded sphere segments of the molecules. The calculated volume by this method should be the same between the trans and cis forms. Also, the electrostriction cannot be so different between these electrically neutral isomers. Therefore, the volume expansion by forming the cis form must be due to an increase in the void volume by bending the molecular structure from a nearly linear structure (Fig. 4). It should be pointed out that the molecular volume of the cis form is considered not to be very much different from that of the trans form in isotropic fluids, because the diffusion constant of the

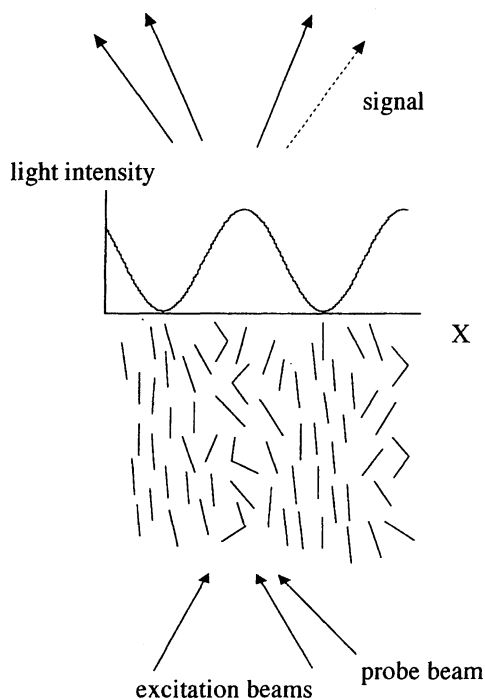


Fig. 4. The cis form produced by the photoisomerization of MBBA induces the disturbance of S and changes the density of the matrix at the same time. The straight and bended lines represent the trans and cis forms of MBBA, respectively.

cis form is nearly equal to that of the trans form in solution.¹⁵⁾ Therefore, the characteristic properties of the nematic phase (the well aligned rod like molecules) may be important for the larger void volume of the cis form.

3. Dynamics of the Density and Order Parameter Changes.

As described in the previous section, there are two contributions in the thermal grating signal: ρ and S . R^{th} of MBBA at room temperature is as large as 7, and the relative contribution of ρ and S is $S : \rho = 8 : 5$ at this temperature. Therefore, by comparing the temporal profile of the e-signal with that of the o-signal, it is expected that the dynamics of the ρ and S can be studied separately. The rise curves after the excimer laser excitation of MBBA probed with the ordi-

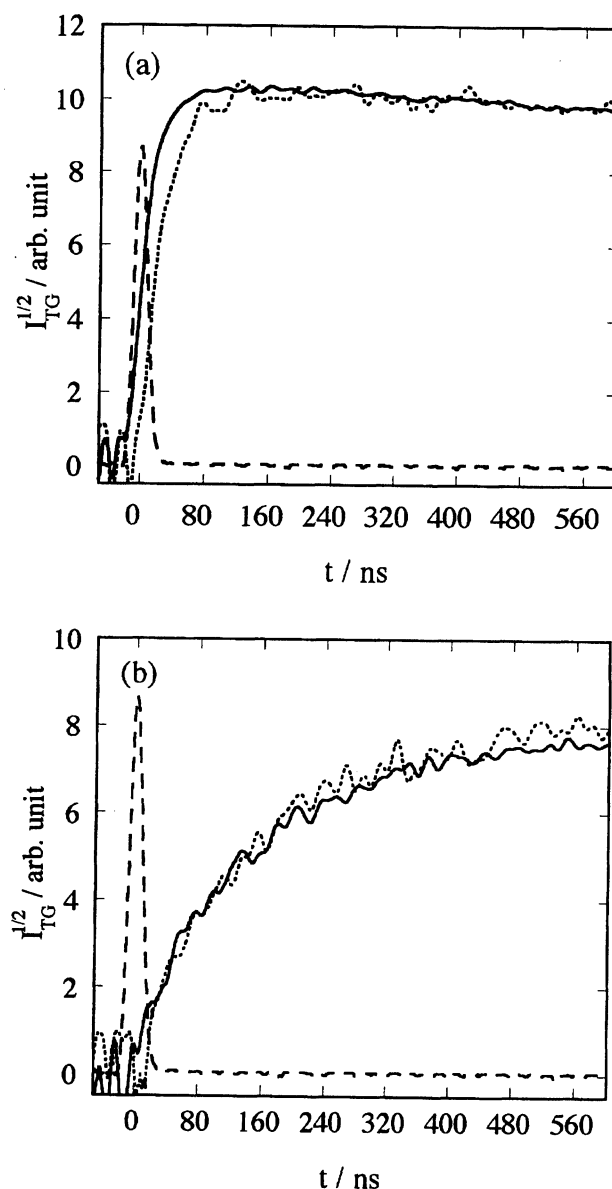


Fig. 5. The rise part of the TG signal of MBBA of the e-signal (solid line) and o-signal (dotted line) at large crossing angle (a) at 21 °C and (b) 44 °C. The signal intensities are normalized. The pulse width of the excitation laser is shown by the broken line.

nary and extraordinary light are shown in Fig. 5. At lower temperatures, both rise curves were significantly different (Fig. 5(a)), while they were very similar at a temperature near the nematic-isotropic phase transition (Fig. 5(b)). The different temporal behaviors at lower temperatures reflect different responses in ρ and S . The similar feature near to the phase transition temperature results from the fact that the S contribution becomes dominant. The slow increase at high temperatures represents a critical slow down of the relaxation process.¹⁾

In order to investigate the build-up time of the ρ and S components in more detail, we studied the rise part of the thermal grating signal of 5CB, which gives only the thermal grating signal upon photoexcitation, because of the lack of the photochemical isomerization. Figure 6 shows the TG signal after the picosecond laser excitation. The acoustic oscillation is clearly observed with a ca. 500 ps period. The acoustic signal observed after the photoexcitation of azobenzene in ethanol is also shown in the figure as a reference. On this time scale, the deactivation of azobenzene is prompt and the heat releasing is considered to be impulsive.²²⁾ As a result, the volume expansion starts from a very early time, and the signal increases with a time constant, that is determined by the acoustic transit time between the fringes. The first peak of the acoustic signal of 5CB appears around 250 ps, which is close to that of the azobenzene in the ethanol sample and also, which reasonably agrees with the calculated acoustic period with v/Λ (v , speed of sound; Λ , fringe spacing). This fact indicates that the heat releasing after the photoexcitation of 5CB is accomplished very quickly (<20 ps). (The slight difference of the oscillation period between 5CB and an ethanol sample is due to the different speeds of sound.)

The notable differences between the o- and e-signals are the intensities and dynamics of the broad background offsets. The offset increases with the delay time between the pump and probe pulses for the e-signal, while it decreases for the o-signal. This offset signal is attributed to the S contribution in the refractive index change, and the temporal profile can be explained as follows. By releasing the thermal energy from the nonradiative transitions within ca. 20 ps after the excitation, the contribution of the density changes starts to increase very rapidly, and at first produces an acoustic oscillation (propagative wave). After several 100 ps, it damps, and the diffusive component (thermal grating signal) remains. On the same time scale, the TG signal due to the S contribution gradually builds up. This component is constructively overlapped to the ρ contribution for the e-signal, but destructively for the o-signal. Therefore, as the S contribution becomes larger, the background offset builds up for the e-signal, but becomes weaker for the o-signal. Although the signal is expected to decay down to the baseline for the o-signal in a sufficiently long time, we could not observe the complete decay because 4 ns is the maximum delay time by our delay stage.

In order to investigate the longer time behavior, we measured the acoustic signal using the nanosecond YAG laser for the excitation and the cw probe with a rather small crossing

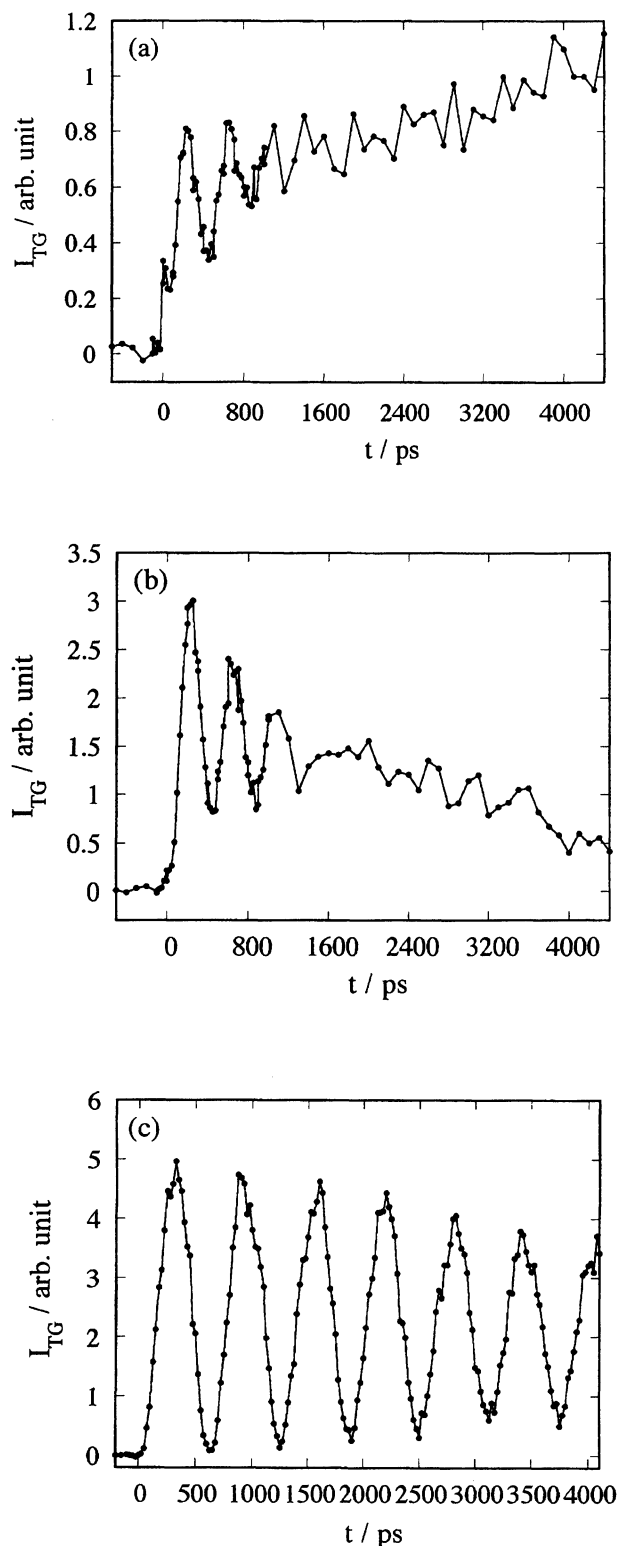


Fig. 6. Temporal profile of 5CB excited by the picosecond laser under the (a) e-signal condition and (b) o-signal condition. (c) Acoustic signal of azobenzene in ethanol under the same conditions.

angle. Figure 7 shows the o- and e-signals of 5CB recorded by the digital oscilloscope. For the e-signal, the acoustic oscillation is dominant at the initial part, and the broad offset

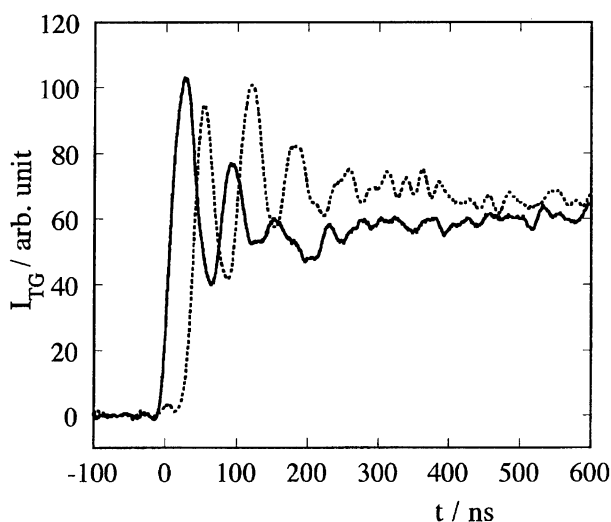


Fig. 7. Acoustic signals of 5CB in nanosecond time scale for the e-signal (solid line) and o-signal (dotted line).

increases at a later time. This behavior of the e-signal is similar to what was observed previously.^{4a,5,7,12} Interestingly, the phase of the acoustic oscillation shifts by about 180° for the o-signal; the peak of the e-signal is the valley of the o-signal. This is explained in terms of destructive interference between the acoustic contribution (ρ) and the background S contribution. We therefore conclude that the S contribution is already dominant within the 10 ns pulse width. The build up time of the S contribution should be somewhere around 5 ns at room temperature under the weak laser-power condition.

Conclusion. Two contributions in the light-induced refractive index change after the real photoexcitation of MBBA and 5CB were studied using the TG method with a polarization selection of the probe beam. In the thermal grating signal, the relative contributions of S and ρ are comparable at room temperature, while the S contribution becomes dominant near to the nematic-isotropic phase transition temperatures. Similarly, two contributions are observed in the population grating signal induced by the photoisomerization reaction of MBBA. One of them is attributed to an S change due to the geometrically distorted molecule (the cis form); the other is due to a density change induced by the void volume of the cis form. The dynamics of the ρ and S contributions were separately studied for 5CB using the acoustic signal from the picosecond to nanosecond time scale.

The author is indebted to Prof. N. Hirota for his helpful discussions and encouragement.

References

- 1) P. G. deGennes, "The Physics of Liquid Crystals," Oxford (1974); H. Kelker and C. Hatz, "Handbook of Liquid Crystals," Verlag Chemie, Weinheim (1980).
- 2) H. Hervet, W. Urbach, and F. Rondelez, *J. Chem. Phys.*, **68**, 2725 (1978).
- 3) a) S. G. Odulov, Yu. A. Reznikov, M. S. Soskin, and A. I. Khizhnyuk, *Sov. Phys. JETP (Engl. Transl.)*, **58**, 1154 (1983); b) **55**, 854 (1983).
- 4) a) I. C. Khoo, *IEEE J. Quantum Electron.*, **22**, 1268 (1986); b) I. C. Khoo, *Phys. Rev., Sect. A*, **23A**, 2077 (1981); c) I. C. Khoo, *Phys. Rev., Sect. A*, **27A**, 2747 (1983).
- 5) J.-C. Khoo and R. Normandin, *IEEE J. Quantum Electron.*, **21**, 329 (1985).
- 6) a) I. C. Khoo, J. Y. Hou, G. L. Din, Y. L. He, and D. F. Shi, *Phys. Rev., Sect. A*, **42A**, 1001 (1990); b) I. C. Khoo, R. R. Michael, and P. Y. Yan, *IEEE J. Quantum Electron.*, **23**, 267 (1987).
- 7) I. C. Khoo, R. G. Liudquist, R. R. Michael, R. J. Mansfield, and P. LoPresti, *J. Appl. Phys.*, **69**, 3853 (1991).
- 8) a) M. Hara, H. Takezoe, and A. Fukuda, *Jpn. J. Appl. Phys.*, **25**, 1756 (1986); b) M. Hara, S. Ichikawa, H. Takezoe, and A. Fukuda, *Jpn. J. Appl. Phys.*, **23**, 1420 (1984).
- 9) S. M. Arakelyan, S. R. Galstyan, O. V. Garibyan, A. S. Karayan, and Yu. S. Chilingaryan, *JETP Lett.*, **32**, 543 (1980).
- 10) B. Ya. Zel'dovich and N. V. Tabiryan, *JETP Lett.*, **30**, 479 (1979); B. Ya. Zel'dovich, N. F. Pilipetskii, A. V. Sukhov, and N. V. Tabiryan, *JETP Lett.*, **31**, 263 (1980).
- 11) H. Hsiung, L. P. Shi, and Y. R. Shen, *Phys. Rev., Sect. A*, **30A**, 1453 (1984).
- 12) H. J. Eichler and R. Macdonald, *Phys. Rev. Lett.*, **67**, 2666 (1991).
- 13) W. Urbach, H. Hervet, and F. Rondelez, *J. Chem. Phys.*, **83**, 1877 (1985).
- 14) S. D. Durbin, S. M. Arakelian, and Y. R. Shen, *Phys. Rev. Lett.*, **47**, 1411 (1981).
- 15) K. Ohta, M. Terazima, and N. Hirota, *Bull. Chem. Soc. Jpn.*, **68**, 2809 (1995).
- 16) E. G. Hanson, Y. R. Shen, and G. K. L. Wong, *Phys. Rev., Sect. A*, **14A**, 1281 (1976); P. A. Madden, F. C. Saunders, and A. M. Scott, *J. Quantum Electron.*, **22**, 1287 (1986); J. J. Stankus, R. Torre, and M. D. Fayer, *J. Phys. Chem.*, **97**, 9478 (1993).
- 17) M. Terazima and N. Hirota, *J. Chem. Phys.*, **95**, 6490 (1991).
- 18) M. Born and E. Wolf, "Principles of Optics," Pergamon, New York (1980).
- 19) H. Kogelnik, *Bell Syst. Tech. J.*, **48**, 2909 (1969); H. J. Eichler, P. Günter, and P. W. Pohl, "Laser Induced Dynamic Gratings," Springer, New York (1986).
- 20) M. Terazima, *Chem. Phys.*, **189**, 793 (1994); M. Terazima, *J. Chem. Phys.*, **104**, 4988 (1996).
- 21) A. Bondi, *J. Phys. Chem.*, **68**, 441 (1964); W. L. Masterton, *J. Chem. Phys.*, **22**, 1830 (1954); J. T. Edward, P. G. Farrell, and F. Shahidi, *J. Chem. Soc., Faraday Trans. 1*, **73**, 705 (1976).
- 22) M. Takezaki, N. Hirota, and M. Terazima, to be published.